CAD Analysis of PCR Well Containment

Manish Deshpande[†], Ken B. Greiner[†], Bart F. Romanowicz[†] , John R. Gilbert[†]
Pamela M. St John[‡] , Timothy Woudenberg[‡]
[†]Microcosm Technologies, 215 First Street #219, Cambridge, MA 02142, manish@memcad.com
[‡]Perkin-Elmer, Applied Biosystems, 850 Lincoln Center Drive Foster City, CA 94404

Abstract

Design analysis of PCR (Polymerase Chain Reaction) microwells are conducted to observe the contamination between neighboring wells on a PCR chip during the reaction. Thermal effects are incorporated to represent the temperature cycling characteristic of PCR. The analyses are intended to be predictive – and to be applied in the design of high throughput PCR devices. Parametric analyses were conducted to observe the effect of the allowable geometry variations on the contamination of the neighboring wells, and the effect of the variation in the diffusivities of the constituent chemical components. The analyses help in developing a set of curves that can be used to develop a model to represent the behavior of the PCR well. This model can then be implemented in system models for the entire device.

Introduction

There is a wide interest in micron-scale integrated chemical/biochemical analysis or synthesis systems, also referred to as lab-on-a-chip [1-3]. On-chip analysis systems consist of active and passive components. Examples of the former are reaction chambers, switching joints etc., whereas the latter include transport and separation channels. The behavior of these components is generally dependent on a number of parameters, including flow conditions and fluid properties. Researchers are forced to use costly trial-and-error experimental methods to understand and design such microfluidic systems.

CAD analyses, on the other hand, can be a valuable aid in the design of microfluidic systems. Numerical analyses provide significant insight into the fluid mechanics in these systems. They also allow the extraction of material and flow properties that are generally not well documented. Such tools help the designer to explore a much larger space of designs than is easily available from experiment, and do so in a quantitative way which enables the extraction of key parameters for improved or optimal operation of common microchemical system components. Finally numerical analyses enable the extraction of component models for each individual component in a system model of the device.

Several researchers have reported CAD-based analyses of microfluidic components [4-6]. These include components used in injection, transport, as well as mixing and reactions. These authors [7-8] have also reported coupled experimental and numerical analyses for various microfluidic components. The component models can be employed in understanding the behavior of the entire device as a system. The value of the system model in understanding the performance of the system is dependent on the ability of the component models in representing the important physics in the component.

An example of a microfluidic device is shown in Fig. 1. The device is designed for high throughput polymerase chain reactions (μPCR). The primary components in this device are the microwells and the interconnects between neighboring wells and to the device loading site. The devices are operated by cycling the temperature to control the PCR reaction. The behavior of the device is characterized by the ability of the wells to contain the sample during the reaction with no leakage into the neighboring wells. The containment is affected significantly by the geometry of the interconnects between the wells and the effect of the temperature cycling on the diffusivity of the sample. Good design of the interconnects aims to minimize the contamination of neighboring wells during the reaction.

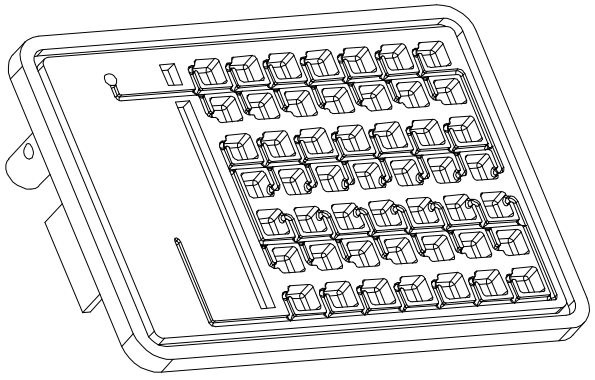

Figure 1: Geometry of Current PCR Chip

Figure 2: PCR Microwell Configurations – Diagonal (left) and Side-by-side (right)

In general, the entire space of design parameters is fairly difficult to analyze experimentally. Numerical methods on the other hand are a viable mechanism – and are the focus of this paper.

We present here a numerical analysis of the PCR wells during the reaction. The effect of the temperature cycling on the diffusivity is considered in the analysis. The effect of varying the cross sectional area of the interconnects is also presented to demonstrate the potential of numerical methods to effectively analyze the design space for these problems. Finally, we will discuss a mechanism of developing a system model for the device.

Device Geometry

The geometry of the current plastic PCR chip is shown in Figure 1. It consists of an array of 49, 1-microliter wells. The nearest neighbor periodicity in the well layout can have two configurations on the chip, as shown in Figure 2: side-by-side (left) or across the diagonal (right). A possibility for a higher density design may consist of an array of 1024 100 nanoliter wells fabricated from silicon using photolithography and an anodically bonded pyrex glass cover to seal the wells. As in the chip in Figure 1, the wells need to be connected to a microchannel running the length of the chip and column and connecting, via a cross channel, to an inlet port.

The PCR chip shown in figure 1 is loaded with different reagents by drying them down in each well using a dispensing robot [9]. The back is then sealed using a polymer tape and the wells are evacuated and then loaded with sample via the inlet port. The device is temperature cycled on a modified research instrument built for real time detection of the µPCR reaction. Details of the temperature cycling are shown Fig. 3. At the outset the system is at room temperature (30 °C). The temperature is then raised uniformly at 4 °C/sec from room temperature to 95 °C and held for 10 seconds. It is then lowered at the same rate to 60

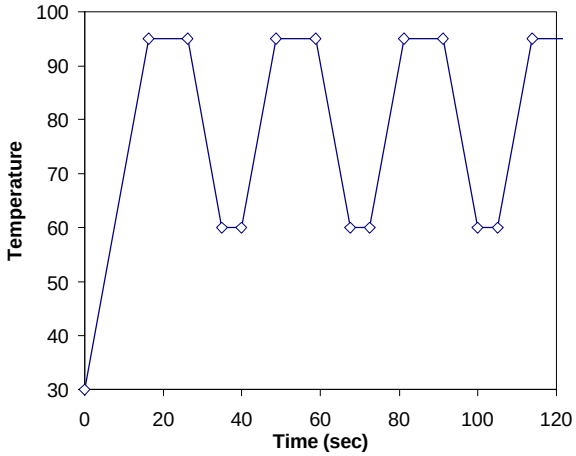

Fig. 3: Temperature Cycling in µPCR wells.

°C and held for 5 seconds. The process then repeats for a total reaction time of 20 minutes. Note that the cycling shown in Fig. 3 repeats for the specified time. Cycling times, in general, are specific for a given device material, volume of sample, and reagent., The times used here are characteristic for microwells and were used in the simulation.

Numerical Analysis

Predictive CAD analyses for the PCR well configurations were conducted to observe the effect of the temperature cycling on the containment of the sample within the well. The leakage into the nearest neighbor well was also analyzed in the process. The different allowable configurations are also studied as part of the analysis. The numerical analyses were conducted using FlumeCAD. FlumeCAD is an integrated design environment consisting of 3D design, modeling and simulation software tools which enable the creation of complex microfluidic devices. Netflow, which is a part of the suite, is specific to the analysis of chemical transport in microchannels. It is an ongoing program, and is a result of a collaboration between Microcosm, Perkin-Elmer Corp. and Stanford University.

The numerical solution of the above equations is performed using a three-dimensional finite element based CFD engine. The Stokes-Einstein formulation was used to determine the diffusivity variation with temperature. Over the cycle used here the diffusivity varies by a factor of about 3. The FlumeCAD interface allows the user to define the geometry from layout and process, or, from a model built in the solid modeler module. Once meshed, the model is available to a suite of solvers for various physical domains, and to the simulation manager to parametrize the dependency in any domain.

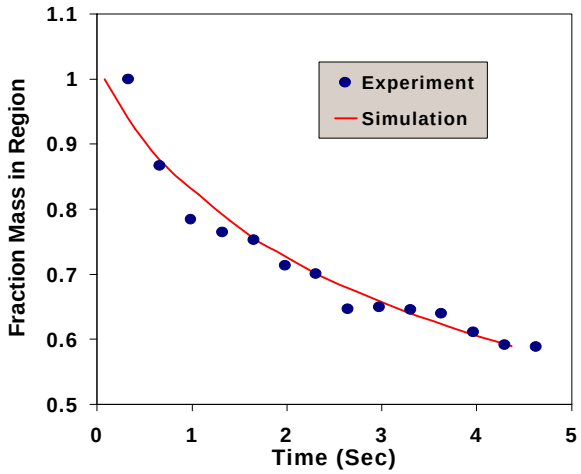

Figure 4: Comparison of Experiment and Simulation for Integrated Mass Leakage out of region.

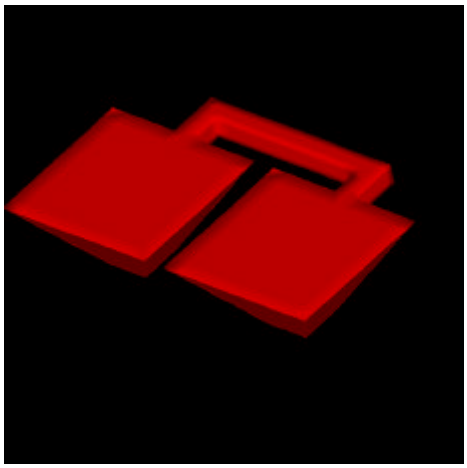

Fig 5: Solid Model of PCR Wells.

Results

Results for the PCR well analysis are discussed in this section. Initially validation of the numerical model is presented, followed by analysis of the different well configurations. Simulations were performed both at ambient temperatures as well as with temperature cycling to compare the difference in containment with temperature cycling in the analysis.

A range of diffusivities is present in the experiment, corresponding to both reactants and products. The lowest diffusivity is 5 e-7 cm2/s, whereas the highest is 1 e-5 cm2/s corresponding to the short chain probe. In the simulations we analyzed diffusivities over this range to ascertain the effect of the various components on the containment in the microwells.

Experimental Validation: To validate our methods, diffusivity experiments were conducted in microchannels to observe the leakage of dye out of a narrow region. The experiments were conducted using fluorescein dye in a straight section of a microchannel (not shown). The comparison between the experiment and simulation, is shown in Fig. 4, and was conducted by digitizing the images and integrating the normalized intensity over a specific region – the integrated intensity corresponds to the amount of dye in the specific region. The agreement between experiment and simulation is good over the entire time sequence, as shown in the figure. This formulation was used to predict the extent of containment during PCR.

PCR Well Simulations: The PCR containment analysis is conducted using the dimensions from the next generation designs. For the purposes of the simulation, detailed analyses were conducted on a reduced configuration,

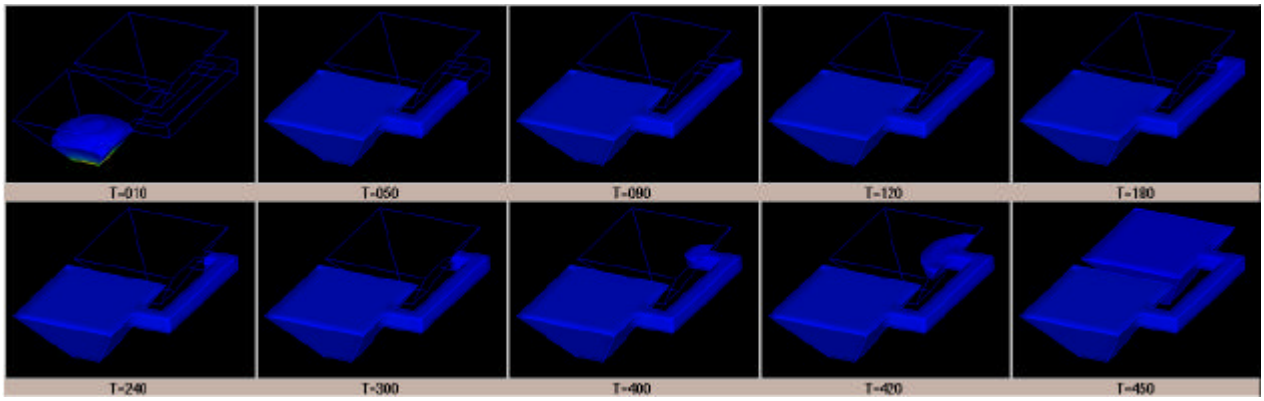

Fig. 6: Species Concentration of Dye in Containment Wells over time. Time increments are in minutes.

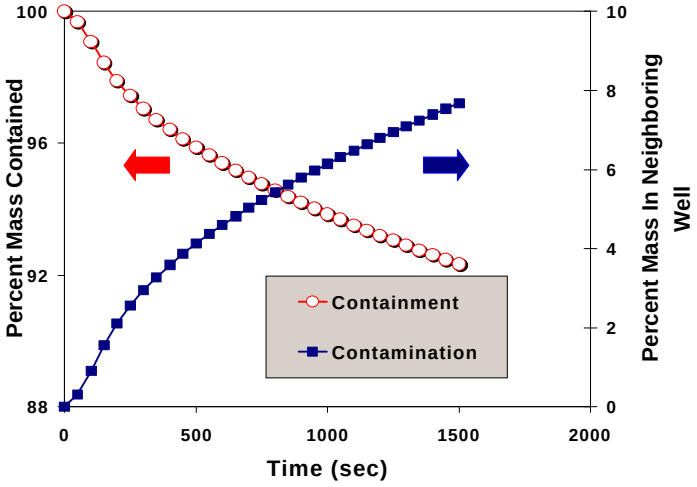

Figure 7: Containment in well during reaction and contamination of Neighboring well.

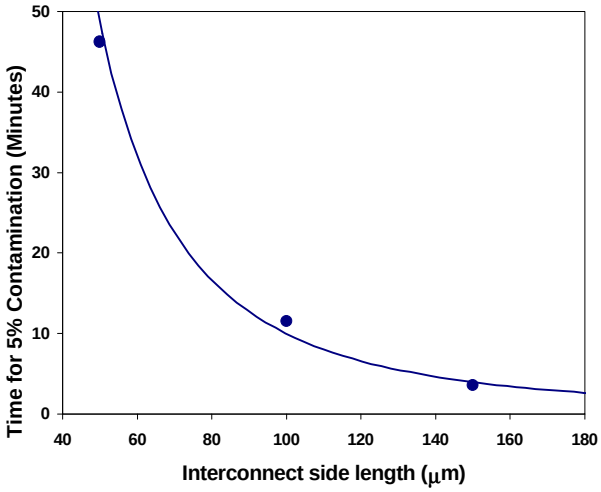

Figure 9: Contamination time as a function of interconnect side length.

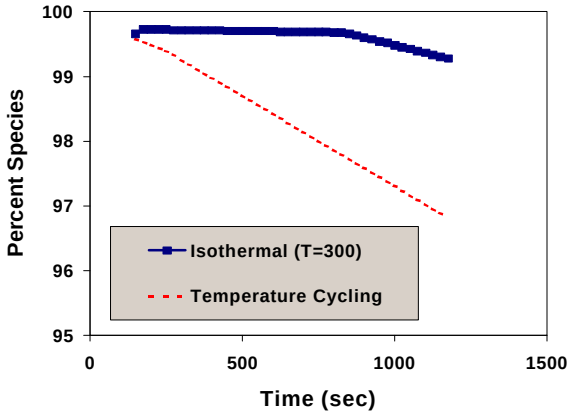

Fig 8: Leakage rate from PCR well with and without temperature cycling

consisting of two nearest neighbor wells. The solid model for this configuration is shown in Fig. 5. This model is adequate to analyze the effects of the temperature cycling and the diffusivity on the containment/contamination characteristics of the design geometry. The problem also becomes considerably more tractable.

Figure 6 shows a simulated timed series of diffusion of material out of a microwell and along an interconnect. The region inside the well is detected during the PCR reaction and therefore, any material which diffuses out of the well in Figure 6 is insignificant providing the material does not diffuse into the neighboring well. Initially, the reactant travels out of the well quickly as it establishes a concentration gradient along the channel. At later times, the solution moves much slower as it diffuses down the channel. Time sequences in the figure are shown for a typical PCR experiment – when allowed to run longer, the species concentrations were predicted to equalize in the two wells in about 8 hours (not shown). The species concentration contained in the well over time is shown in Figure 7. The concentration entering the neighboring well is also shown in the figure. These curves were computed using a Region-of-Interest (ROI) integration over the wells after the computation. The ROI integral is then analogous to the collected signal in a detection system for the well. A curve such as Fig. 7 is an important asset in the design of these devices since it indicates the allowable reaction times that prevent contamination of reagents (and therefore the reaction) between neighboring wells.

The effect of incorporating the temperature cycling is shown in Figure 8. The leakage rate from the chamber is compared with the results of the simulation at constant temperature. The diffusion constant in the isothermal case was taken to be constant at the room temperature value. A different constant temperature value would yield a shift in the leakage rate, but would still be inaccurate in comparison to the variable temperature results. As the figure shows the temperature cycling and the correspondingly higher diffusivity has a dramatic effect in increasing the leakage rate from the reaction chamber. This figure also serves to highlight the importance of including the relevant physical processes into the computation since the presence of the temperature cycle significantly alters the design analysis for the problem.

Effect of interconnect geometry: The cross sectional area of the interconnect can also have a significant effect on the contamination time between the wells. Computations were conducted using the Simulation Manager in FlumeCAD to analyze the effect of the allowable variations in the design. Results are presented in Fig. 9, showing the contamination time for the different configurations. The contamination time

here was defined as the amount of time required for 5 percent of the species in the first well to enter the neighboring well. As the figure shows, for the highest (150 μm) case, contamination occurs well within the specified reaction time. For a side length of 100 μm as well, contamination occurs at approximately 10.5 minutes, which is within the reaction time. For a 70 μm side length, however, the contamination time increases to over 22 minutes, implying that it is a more appropriate choice for the interconnect cross sectional dimension.

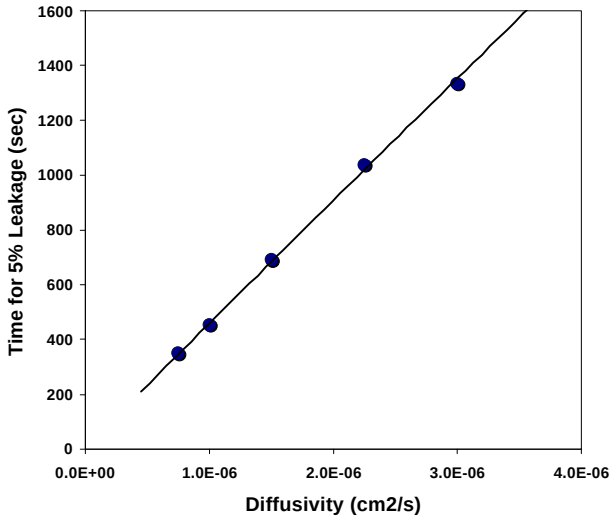

Figure 10: Contamination time as a function of diffusivity.

Effect of Diffusivity: In the course of the PCR reaction the diffusivities observed for the sample, enzyme and product mixture range from about 5e-7 cm2/s to about 1e-5 cm2/s. The rate of contamination is strongly dependent on the diffusivity. However a full reaction analysis for PCR is computationally intensive – and is not entirely required for design analysis. We demonstrate this here, by studying the effect of the diffusivity on the contamination. In general the contamination times lie between that for the highest and the lowest diffusivity – the design can then be tailored for an appropriate specification. The contamination time has a linear dependence on the diffusivity as seen in Figure 10 – appropriate leakage rates for specific diffusivities can then be extracted from this curve.

Curves such as Figures 7-10 describe the behavior of the PCR wells as a component in the overall PCR system. This behavior can be used to develop an appropriate reduced-order model for the wells – this model can be implemented in a system model for the PCR system. The implementation of the system model is the focus of our current research.

Conclusions

Detailed analyses of PCR well configurations were conducted to predict the contamination between neighboring wells during a conventional PCR cycle. Temperature dependent effects from the thermal cycling were incorporated using appropriate diffusion models. The contamination time was computed as the time required for 5 percent sample travel between neighboring wells. The effects of the cross sectional geometry as well as the diffusion constants of the various components in the mixture were analyzed through simulation. The parametric results yielded curves that describe the contamination between wells in terms of the various parameters that affect it. These curves can then be applied in developing optimal designs for the wells, as well as in the development of a model describing the behavior of the PCR well as a function of the various parameters affecting it. This model can then be implemented in a system model for the entire device, and is the focus of our current work.

Acknowledgements

This work was funded by DARPA Composite CAD (Grant no. F30602-96-0306), under the Netflow Program.

References:

[1] D.J. Harrison, et al, *Science*, **261** (1993) 895-897.
[2] Luc Bousse, Bob Dubrow and Kathi Ulfelder, *u-TAS '98*, 271.
[3] N. Chiem and D.J. Harrison, *Anal. Chem.*, **69** (1997), 373.
[4] X. C. Qui, L. Hu, J. H. Masliyah, and D. J. Harrison, *Solid-State Sensors and Actuators*, Chicago, IL (1997).
[5] N. A. Patankar and H. H. Hu, *Anal. Chem.*, **70**, (1998).1870-81.
[6] Sergey V. Ermakov, S.C. Jacobson, and J.M. Ramsey, *u-TAS '98*, 149.
[7] P.M. St. John, et al, *Solid State Sensors and Actuators Workshop*, Hilton Head, SC (1998).
[8] M. Deshpande, et al, MEMS '99, Orlando, FL.
[9] M. Albin, et al, *Solid State Sensor and Actuator Workshop*, 2 June (1996).